Pharmaceutical Research, Vol. 23, No. 1, January 2006 (© 2006)
DOI: 10.1007/s11095-005-8636-3

Research Paper

Kinetics of Insulin Adsorption at the Oil–Water Interface and Diffusion Properties of Adsorbed Layers Monitored Using Fluorescence Correlation Spectroscopy

Jesper Donsmark,[1,2,5] Lene Jorgensen,[3] Susanne Mollmann,[3] Sven Frokjaer,[3] and Christian Rischel[1,4]

Received December 2, 2004; accepted September 19, 2005

Abstract. The adsorption of insulin at an oil–water interface was studied with fluorescence correlation spectroscopy (FCS). FCS is able to measure diffusion properties of insulin at nanomolar concentrations, making it possible to detect the very early steps in the adsorption process. Below 20 nM bulk insulin concentration, the insulin molecules adsorbed to the surface diffuse freely at all times during the experiment (a few hours). At higher concentrations, a surprisingly abrupt transition to a slow diffusion phase is observed. Based on the information about both diffusion times and molecular brightness derived from the FCS experiments, we suggest that the transition represents the formation of a fractal network. FCS may be a valuable tool in pharmaceutical formulation science, because it provides information about concentration buildup and phase changes at interfaces formed in drug delivery systems.

KEY WORDS: adsorption; fluorescence; fluorescence correlation spectroscopy; insulin; oil–water interface.

INTRODUCTION

In the development of drug delivery systems containing protein drugs, the behavior of proteins at various interfaces has been the subject of increasing interest. A liquid–liquid interface is present in several drug delivery systems, e.g., emulsions and microspheres. Proteins adsorb to interfaces (1), which often results in structural changes (2) that may affect the biological activity and physical/chemical stability of the protein (3–5). To be able to optimize their function in drug delivery systems, information about the behavior at the interfaces created in drug delivery systems must therefore be obtained. A micropipette technique was recently used to study the surface formed at the interface between oil and a protein solution (6). In these experiments a condensed film was formed at the surface of the droplets.

In the present work, we studied the initial steps in the formation of the protein film by confocal fluorescence correlation spectroscopy (FCS). FCS is a technique that in recent years has become commercially accessible and has since significantly contributed to the field of molecular biology. The main strength of the technique is its ability to determine the diffusion constant, concentration, and brightness of fluorescent molecules (7). The dissociation constants and on/off rates of C-peptide to human cell membranes were measured by Rigler *et al.* (8), and the dynamics of β_2-adrenergic receptor–ligand complexes was recently measured on living cells (9). Schmauder *et al.* (10) demonstrated how FCS may be used to screen for crystallizing conditions in protein solutions. To our knowledge, diffusion of proteins at the oil–water interface has not been previously studied via FCS, although it provides a model system for two-dimensional diffusion. The use of confocal microscopy opens up the possibility of detecting fluorescent-labeled particles directly at the oil–water interface, because the detection volume can be positioned with submicrometer precision.

Interest for studying adsorption of insulin at hydrophobic surfaces is mostly based on the use of the protein in various drug delivery systems (11). The focus has mainly been on interactions of insulin with solid–liquid interfaces occurring in pump devices (12–15); however, the interaction with liquid–liquid interfaces created in various drug delivery systems is also of interest. Human insulin is a small protein consisting of 51 amino acids distributed in two polypeptide chains, the A and the B chains (16), with a total MW of 5.8 kDa. The insulin monomer has a rather hydrophobic surface and it spontaneously associates into dimers and at higher concentrations into tetramers and hexamers (17). Hexamers of insulin are stored in the body in a complex with Zn ions, which stabilize the hexamer even further (16). As monomeric and dimeric forms are the most hydrophobic species, they are expected to be the ones to adsorb (11,12).

[1] Niels Bohr Institute, University of Copenhagen, Copenhagen, Denmark.
[2] Department of Biophysics, Leiden University, Leiden, The Netherlands.
[3] Department of Pharmaceutics, The Danish University of Pharmaceutical Sciences, Copenhagen, Denmark.
[4] Novo Nordisk, Novo Allé 6A, DK-2880, Bagsværd, Denmark.
[5] To whom correspondence should be addressed. (e-mail: donsmark@physics.leidenuniv.nl)

The main objective of the present study is to evaluate FCS as a method of studying the early steps in the adsorption process of insulin at the oil–water interface. In the FCS experiments, insulin labeled with fluorescein isothiocyanate (FITC) was used. The fluorescent label is bulky, and this may impair the association of FITC–insulin into hexamers due to steric hindrance; however, dimers can still be formed (18). The impaired hexamer formation is not considered of importance, because only the monomer is present at the concentrations used (19,20).

MATERIALS AND METHODS

Materials

Recombinant human insulin (purity 98.7%) contained 2 Zn^{2+} per hexamer and was kindly donated by Novo Nordisk (Bagsværd, Denmark). Fractionated coconut oil (Miglyol 812), which is a medium chain triglyceride oil (MCT oil), was kindly donated by H. Lundbeck (Copenhagen, Denmark). The triglyceride contains at least 98% C8 and C10 fatty acids and has an acid value of 0.03. Fluorescein isothiocyanate (FITC) was obtained from Molecular Probes (Leiden, The Netherlands). All other chemicals used were of analytical grade.

Methods

Preparation of Monolabeled FITC–Insulin

Human insulin was monolabeled with fluorescein FITC following the procedure described by Hentz *et al.* (21). FITC solution was added drop wise to 2 mL of insulin solution (10 mg/mL), resulting in a molar ratio of 1:1. The solution was protected from light and incubated for 20 h on an end-over-end rotator. The reaction was stopped by placing the mixture on a gel filtration column (Superdex 75; Amersham Biosciences, Uppsala, Sweden), which was preequilibrated with phosphate buffer (HNa_2PO_4/H_2NaPO_4; 10 mM, pH = 7.4). The column was protected from light. The first peak detected by UV (280 nm) was collected in fractions of 1 mL and analyzed by MALDI-TOF (data not shown). Only fractions where the major part of the protein (>90%) was monolabeled were pooled and used for the fluorescence experiments. The concentration of FITC–insulin was determined on a UV spectrophotometer by the BCA method (22).

Microscopy at Oil–Water Interfaces and FCS Measurements.

Chambered cover glasses (Labtek-II; Nunc, Roskilde, Denmark) were cleaned by filling with 3% HF and incubating for 30 s. The cover glasses were rinsed with Milli-Q water and dried in a stream of Nitrogen gas. They were subsequently stored for up to 30 days. Before the experiments, the cover glass well was filled with 5% HNO_3 and incubated for 15 min, rinsed in Milli-Q water, and dried with nitrogen gas. This procedure ensures that oil droplets form symmetric spherical droplets on the glass surface and reduces insulin adsorption to the glass. All insulin solutions were made from 10 mM phosphate buffer at pH 7.4. FCS measurements were performed with a confocal microscope equipped with an FCS unit (Confocor2; Carl Zeiss, Jena, Germany (23)), as illustrated in Fig. 1. Samples were illuminated at 477 nm and fluorescence was detected through a band path filter (530–560 nm). This combination of excitation and emission wavelengths gave a good signal from the FITC probe and low background from the oil. A Zeiss 40×1.15 NA objective and a pinhole with the width of an airy disk was used.

To set up the oil–water interface, 1 μL of oil was applied to the bottom of a cover glass chamber and dispersed with a pipette tip. The oil then spontaneously formed tiny drops on the surface. Next, 500 μL buffer was added and the built-in camera was used to locate the apex of an oil droplet (diameter = 20–40 μm), using the reflection from the oil–water interface. Afterwards, a mixture of FITC–insulin and unlabeled insulin was added. The concentration of FITC–insulin was 3 nM in all experiments, whereas the amount of unlabeled insulin was varied. The confocal volume was then repositioned at the apex to correct for shifts in the oil droplet position during mixing. The position of the interface is continuously drifting (typically 3 μm/h). This was compensated by repositioning of the detection volume between measurements; the interface drift is small enough to allow stable measurements on the time scale of FCS measurements. Typically, data were collected for 6×20 s

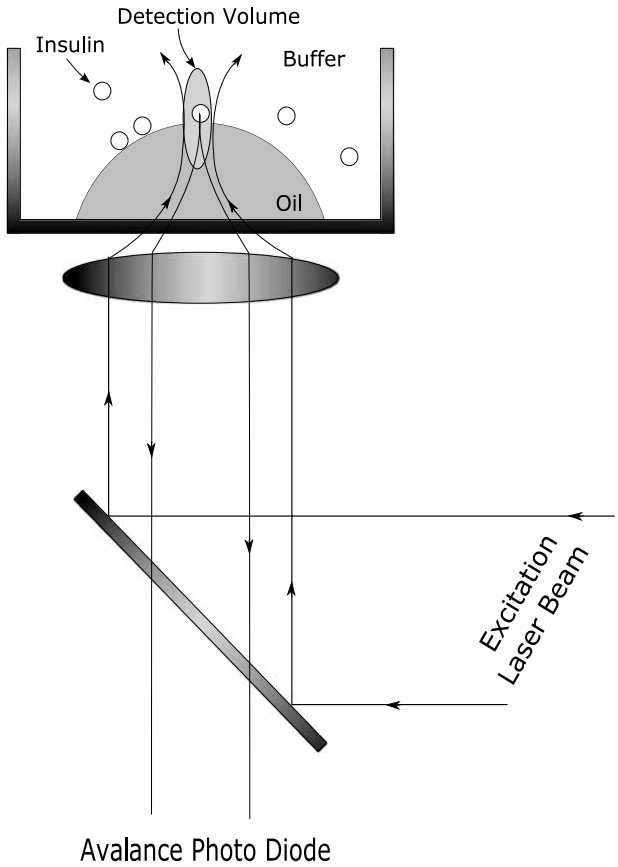

Fig. 1. Sketch of experimental setup (not drawn to scale). Oil droplets are located on a chambered coverslip filled with buffer and FITC-labeled insulin. A laser beam is focused onto the interface region at the apex of a selected oil droplet. The objective collects the fluorescence, which is detected by a photodiode. For more complete description of the optical instrumentation, see (23).

and the autocorrelation function was averaged. Depending on the drift velocity of the interface, the z-position of the detection volume was adjusted manually within a 20-s interval and the autocorrelation function of these data were discarded from the average. For experiments with high concentrations of insulin ($C > 75$ nM), autocorrelation functions from single traces of 20 s were used.

Confocal Scanning Imaging and Vertical Fluorescence Scans

Fluorescence intensity scans in the vertical direction were recorded using the micropositioning stage. Confocal scanning images were recorded using the LSM unit of the microscope. Images of 512×512 pixels were recorded using a scanning time of 8 s. For illumination, the 488-nm line was used in conjunction with a 505-nm-long path filter.

RESULTS and DISCUSSION

The aim of this study was to evaluate FCS as a tool to study the adsorption process of proteins at the oil–water interface. A discussion on the application of FCS oil–water interfaces is given followed by a discussion of the results.

FCS Applied to Measurements at Interfaces

The highly sensitive photodiode used in FCS enables the detection of single photons from fluorescent molecules diffusing through the confocal detection volume, which has the size of about 1 fL. The fluorescence autocorrelation function $g(\tau)$ is calculated from the time-resolved series of photon detection events using the multiple tau algorithm (24). Analysis of the autocorrelation function requires an assumption about the geometry of the detection volume. In bulk measurements, i.e., in a buffer, where no interfaces are present, the fluorescence detection volume can be approximated with a Gaussian volume (25). This assumption allows the calculation of the correlation function for a single diffusing species, taking into account the three-dimensional geometry:

$$g_{\mathrm{D}}^{3\mathrm{D}}(\tau) = \frac{1}{N\left(1+\frac{\tau}{\tau_{\mathrm{D}}}\right)\sqrt{1+\frac{\tau}{\tau_{\mathrm{D}}S^2}}} \tag{1}$$

Here, N is the average number of particles in the detection volume and τ_{D} is the characteristic diffusion time, which is the average residence time of molecules in the detection volume. The structure factor $S = \omega_{\mathrm{V}} / \omega_{\mathrm{H}}$ is the ratio between the vertical and horizontal widths of the detection volume. The diffusion time depends on ω_{H} and the diffusion constant of the molecule studied:

$$\tau_{\mathrm{D}} = \frac{\omega_{\mathrm{H}}^2}{4D} \tag{2}$$

Hence, the size of the confocal spot in bulk solution can be estimated by measurements on a molecule with known diffusion constant. In our setup, the diffusion time of Tetramethylrhodamine, which has a diffusion constant of 2.8×10^{-10} m^2/s (26), is 30 μs. This allows an estimation of the horizontal width of the detection volume according to Eq. (2) and gives a confocal spot area ($\pi\omega_{\mathrm{H}}^2 / 4$) of 0.03 μm^2.

In reality, the detection volume of a confocal microscope shows considerable deviations from the Gaussian shape (27), in particular in the longitudinal direction (along the beam). In the case of FCS, the Gaussian approximation to the autocorrelation function was extensively tested for bulk (three-dimensional) diffusion and shown to be reasonable (25,28,29). If the fluorescent particles are constrained to diffuse on a surface approximately perpendicular to the beam, the three-dimensional geometry breaks down into a two-dimensional geometry and one obtains:

$$g_{\mathrm{D}}^{2\mathrm{D}}(\tau) = \frac{1}{N\left(1+\frac{\tau}{\tau_{\mathrm{D}}}\right)} \tag{3}$$

With the detection volume now only a thin, transverse slice of the 3D volume, we expect the Gaussian approximation to be very good. The size of the detection area might be modified by the passage of the light through the oil drop in our geometry (30).

Apart from fluctuations due to Brownian motion, the intensity may change because of the photophysics of the dye, which also contributes to the correlation function. Dye molecules may decay from the excited state via a nonfluorescent triplet state. Widengren and Rigler (31) showed how the decay may be incorporated into the autocorrelation function as shown in Eq. (4).

$$g(\tau) = g_{\mathrm{D}}(\tau) g_T(\tau) \tag{4}$$

where $g_{\mathrm{T}}(\tau)$ is the triplet contribution to the autocorrelation function and reads:

$$g_T(\tau) = 1 - T + T\exp\left(-\tau/\tau_{\mathrm{T}}\right) \tag{5}$$

T is the fraction of molecules in the triplet state and τ_{T} is the characteristic triplet time (31).

Bulk measurements of FITC-labeled insulin show a diffusion time of about 60 μs (data not shown). With high powers of excitation, a 2-μs decay component was seen, due to population of the triplet state. Figure 2 shows the autocorrelation function from surface measurements of FITC–insulin freely diffusing at the water–oil surface at a bulk concentration of 20 nM. The decay of the autocorrelation function takes place on three timescales. The fastest has a decay time on the order of a few microseconds and is attributable to population of the triplet state. The slowest decay must be assigned to diffusion of the molecules along the interface and has a diffusion time on the order of 2000 μs. A similar increase (30×) in the diffusion time of protein ovalbumin upon adsorption to an air–water surface was observed by Kudryshova *et al.* (32). It is possible that in reality the particles at the surface display a distribution of diffusion times, but our data are well described by a single component.

The intermediate regime decays on the order of 100 μs, which is comparable to the diffusion time of bulk insulin. It would be a plausible explanation as the detection volume is expected to penetrate several hundred nanometers into the bulk solution. The fit to this model, as shown in Fig. 2A, gives

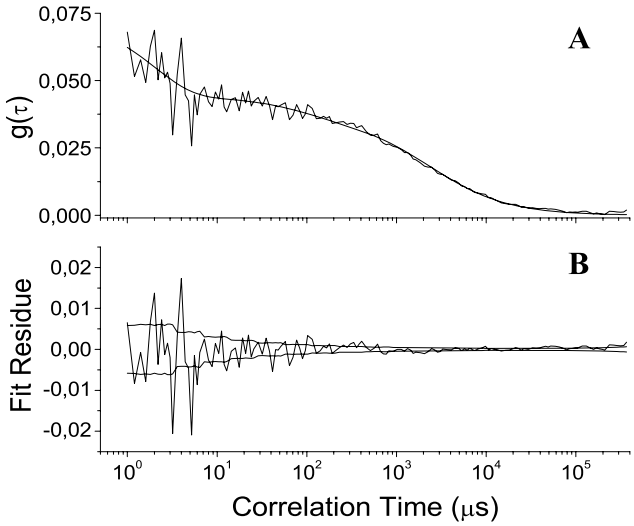

Fig. 2. The autocorrelation function of 20 nM insulin diffusing at the oil–water interface. The residual from the fit to Eq. (6) is shown in panel B. The thick line, describing a step-like function, is the standard deviation of a master curve (see text for details) and has been used to weight the fit data points as described by Wohland *et al.* (35).

a reasonably good agreement with data on all time scales. The formula is given in Eq. (6).

$$g(\tau) = g_T(\tau)\left(a_b g_D^{3D}(\tau) + a_s g_D^{2D}(\tau)\right) = (1 - T + T\exp(-\tau/\tau_T)) \times \left(a_b \frac{1}{\left(1+\frac{\tau}{\tau_{Bulk}}\right)\sqrt{1+\frac{\tau}{\tau_{Bulk}S^2}}} + a_s \frac{1}{\left(1+\frac{\tau}{\tau_{Surface}}\right)} \right) \quad (6)$$

In this interpretation of our data, the two amplitudes, a_b and a_s, depend on the number of particles in bulk volume and on the surface within the detection volume. If the brightness of fluorescence is the same for FITC–insulin on the surface and in the bulk, amplitudes a_b and a_s can be directly related to average particle numbers within the confocal volume. Our estimates obtained in this manner of the bulk concentrations outside the interface in several cases significantly exceed the concentration originally added to the sample. Because this is not physically plausible, the number of particles calculated from the amplitudes are probably biased by a brightness difference between the two diffusion species, as previously reported by Palo *et al.* (33). However, in the same study, it is shown that FCS measures the diffusion time reliably in systems of mixed species, when the diffusion time of one the components is known in advance and fixed during the fitting procedure. Therefore all data were fitted using Eq. (6) with certain parameters fixed to the value measured from insulin diffusing in bulk solution: bulk diffusion time (τ_{Bulk}), structure parameter (S), and triplet time (τ_T). The fit thus gives the surface diffusion time $\tau_{Surface}$ and the particle numbers $N_{Surface} = a_s / (a_s + a_b)^2$ and $N_{Bulk} = a_b / (a_s + a_b)^2$. As explained above, the particle numbers might be biased by differences in brightness.

Data fitting was performed using a nonlinear minimization (Nelder–Mead) (34) and for weighing we employed a modified version of the method described by Wohland *et al.* (35), which uses the standard deviation of FCS curves as a weight function. A single master curve of the standard deviation, created from 720 scans of 20-s duration from freely diffusing R6G dye, is shown in the residual plot in Fig. 2B.

Under the assumption that the surface affinity is the same for FITC–insulin and unmodified insulin, the total number of labeled and unlabeled insulin particles (N^{Total}) can be calculated from the detected number of fluorescent particles measured with FCS (N^{FITC}) and the ratio of FITC–insulin to the total concentration of insulin:

$$N_{Surface}^{Total} = N_{Surface}^{FITC} \frac{C_{Bulk}^{Total}}{C_{Bulk}^{FITC}} \quad (7)$$

Although FITC alone at most weakly associates with the surface (Figs. 3D and 4), significant change in the affinity of insulin upon labeling can not be completely ruled out. This would shift the calculated numbers by a constant factor.

The fitted number of particles ($N = N_{Surface} + N_{Bulk}$) can be combined with the detected intensity (I) to calculate the average brightness (B) of the molecule, cf. Eq. (8).

$$B = \frac{I}{N} \quad (8)$$

The brightness is useful for detecting a dimerization and higher degrees of association of particles, as more particles

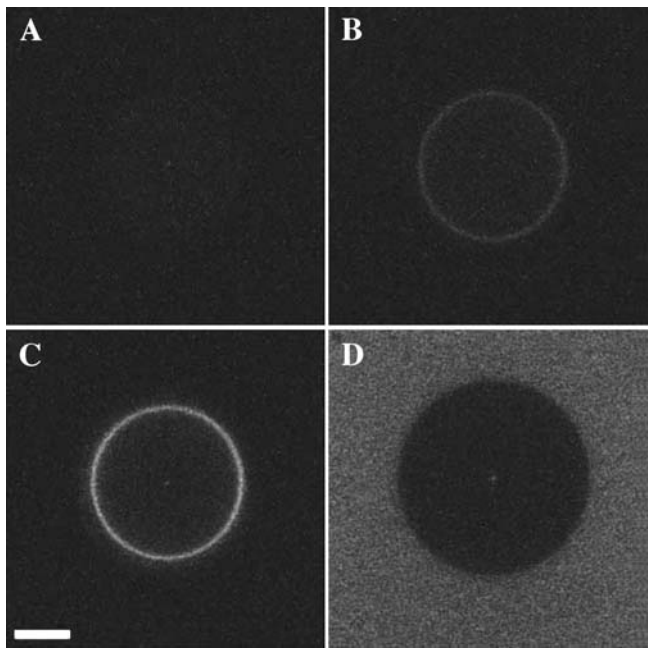

Fig. 3. The adsorption process of FITC–insulin studied by confocal scanning microscopy. The fluorescence intensity of oil droplets submerged in buffer, FITC–insulin, and FITC–dye has been measured. (A) Oil droplet in buffer shows no increase in intensity at the oil–water interface. (B) Thirty seconds after addition of 3 nM FITC–insulin, fluorescent protein accumulates at the surface. (C) Fifteen minutes after FITC–insulin addition, the fluorescence signal increases further. (D) A new oil droplet incubated with 30 nM FITC–dye for 15 min. Enhancement of the intensity at the interface is absent. Scale bar (C) = 10 μm.

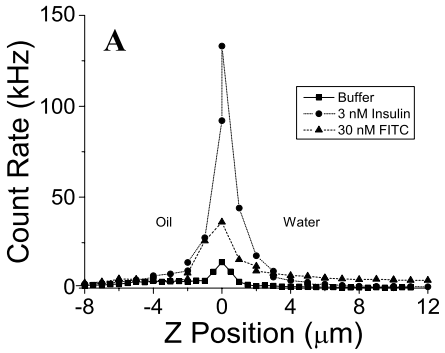

Fig. 4. Fluorescence intensity scanned on a vertical plane after incubation for 15 min. Three scans of droplets incubated in buffer, buffer with FITC–insulin, and buffer with FITC–dye have been overlaid with the oil–water interface positioned at $z = 0$ μm. FITC–insulin (3 nM) gives a significant fluorescence signal at the surface compared to FITC–dye (30 nM), whose intensity is more comparable to the scattering signal of the buffer.

diffusing together gives a lower number of particles at the same total intensity, although care must be taken when interpreting the brightness, because aggregation may also affect the quantum yield of the dye.

FITC is known to be susceptible to photobleaching. Bleaching during measurements will show up as an additional decay in the autocorrelation function (31). We experimentally observe correlation functions with characteristic times in excess of 100 ms, which sets a high lower limit on the bleaching time. We have therefore not included this component in the analysis.

Adsorption Properties of FITC–Insulin

Confocal scanning images have been used to give a qualitative visualization of FITC–insulin adsorption to the oil interface. The image of an oil droplet in pure buffer are shown in Fig. 3A, where the addition of 3 nM FITC–insulin yields a fluorescence signal from adsorbed protein at the oil–water interface. Figure 3B and C shows the images recorded after 30 s and 15 min, showing that the fluorescence clearly increases within the applied time frame. Figure 3D shows the result of an experiment where 30 nM pure FITC dye was added to an oil droplet in buffer. No surface adsorption is observed, indicating that pure FITC has significantly lower affinity for the oil–water surface than the labeled insulin.

Vertical fluorescence intensity scans shown in Fig. 4 give information about the spatial localization of fluorescent molecules at the oil–water interface. This can be used to compare the binding affinity of FITC and FITC–insulin to the interface. The intensity detected at the surface comes from various sources: fluorescence from adsorbed molecules, from bulk fluorescence, and from scattering due to the shift of refractive index at the oil–water interface. In pure buffer, there is a small signal of 15 kHz detected at the interface, which can be attributed to scattering as a result of the refractive index change. Adding 3 nM FITC–insulin gives a signal of 130 kHz, whereas the addition of the 30 nM FITC dye alone gives a peak of 35 kHz. This indicates that binding of FITC–insulin the interface is not attributable to the label, but mainly a property of insulin itself.

FCS Measurements of Insulin at the Oil–Water Interface

FCS measurements allow operators to follow the concentration and diffusion time of insulin at the oil–water interface on the time scale ranging from minutes to hours. Figure 5 shows the diffusion time and number of particles as function of time for typical experiments at different bulk concentrations. At the first time point, the adsorbed layer has a characteristic diffusion time on the order of 1.5–2 ms for all concentrations. For concentrations $C_{\mathrm{Bulk}} \geq 20$ nM, the diffusion time starts to increase during the measurement, and at a certain point it moves out of the measurable range. Rather than a gradual increase, we always see a very abrupt surge in the diffusion time. This points to an interesting change in environment or conformational rearrangement of insulin. The rate of formation of this slow diffusion phase seems to be highly dependent on the bulk concentration used. We somewhat arbitrarily define the formation rate κ_{Slow} of the slow phase as the reciprocal of the time $t_{15\ \mathrm{ms}}$ it

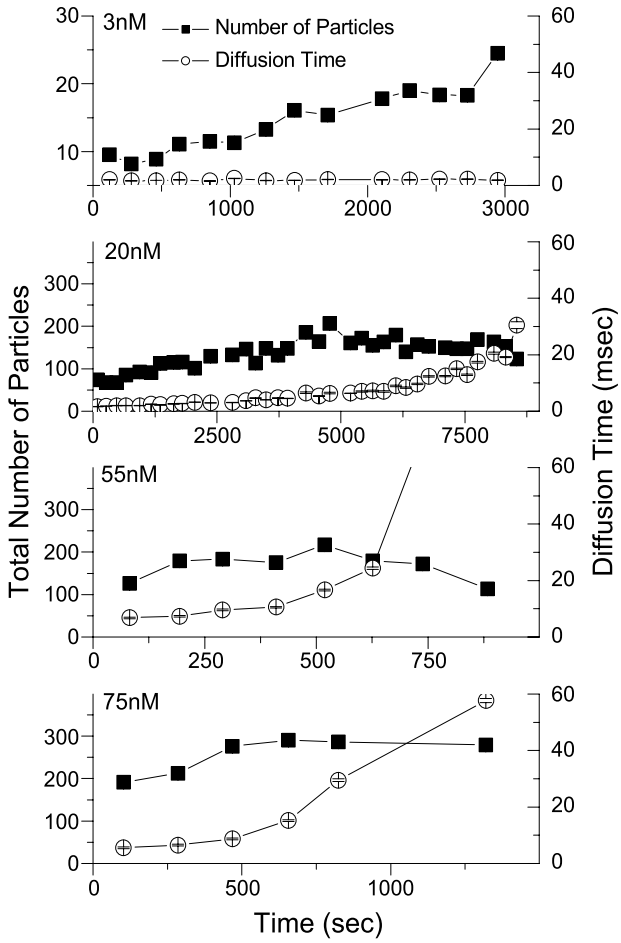

Fig. 5. The number of particles in the confocal volume and the characteristic diffusion time as function of time for several concentrations. A mixture of labeled and unlabeled insulin was used. The total concentration was varied, whereas labeled insulin constituted 3nM. Each experiment was repeated at least twice and a representative graph is shown.

takes before the diffusion time (τ) reaches 15 ms, which is approximately ten times the initial surface diffusion time.

$$\kappa_{\text{Slow}} = \frac{1}{t_{15\text{ms}}} \tag{9}$$

As the diffusion time increases steeply at this point, the results are changed very slightly by choosing a different threshold. The immobilization rate obtained from Eq. (9) is plotted in Fig. 6 and describes an increasing function.

The first data in the time series were collected after 90±20 s after addition of insulin. It can be seen in Fig. 5 that the surface concentration only grows slowly, if at all, after this time. This shows that the sudden slowing of the surface mobility does not happen in response to a threshold concentration being reached, but rather as the result of a maturation process proceeding at nearly constant concentration. There is a very large variation of 50% or more in the initial number of fluorescent particles even between supposedly identical experiments. We do not presently understand the source of this variation, which precludes detailed quantitative analysis of the surface concentration. For low total bulk concentrations (insulin + FITC–insulin), the number of fluorescent particles accumulated in the detection volume at the first time point is 11±3. Assuming spherical symmetry, the number of molecules needed to achieve this surface concentration can be calculated to be contained within a distance of ~50 μm. A rough estimate of the time required for these particles to diffuse to the surface is $t = 4Dd^2$, where d is the distance. This gives a time of less than 10 s. Hence, the surface concentration is established well before the first data points are collected, and is thus only dependent on bulk concentration. After the initial equilibrium between bulk and loosely adsorbed insulin is established, surface concentration increases with time for low concentrations ($c_{\text{Bulk}} \leq 20$ nM), whereas the surface seems to be nearly saturated at higher concentrations. The later adsorption, seen at low concentrations, can be interpreted as a secondary transition to a state with higher binding affinity.

$$C_{\text{Bulk}} \overset{\text{Fast}}{\longleftrightarrow} \Gamma_{\text{Surf}}^{\text{Loose}} \overset{\text{Slow}}{\longleftrightarrow} \Gamma_{\text{Surf}}^{\text{Tight}} \tag{10}$$

The surface concentration increases until equilibrium between loosely adsorbed insulin and tightly adsorbed insulin is obtained. For concentrations $C_{\text{Bulk}} \leq 20$ nM, the adsorption levels out at surface concentrations of $N_{\text{Surface}}^{\text{Total}} = 150 \pm 20$. At higher bulk concentrations the surface concentration only increases weakly and seems to be nearly saturated at the beginning of the experiment.

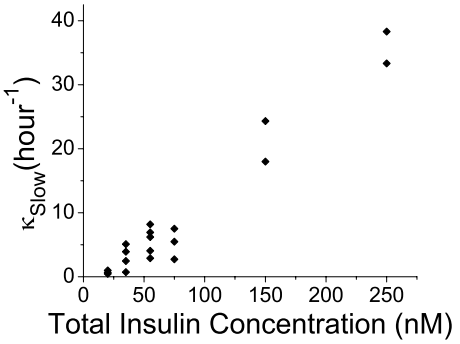

Fig. 6. The rate of formation of the slow diffusion phase vs. the total concentration of labeled and unlabeled insulin in bulk. The rate was calculated according to Eq. (9).

The increase in diffusion time is accompanied by a decrease in the number of fluorescent particles. This can be attributed to photobleaching of the dye. The increased diffusion time gives each molecule a longer residence time and irradiation exposure in the detection volume. Photobleaching is generally observed as a decrease in the count rate during acquisition. We measure stable intensity traces until the point where the diffusion time increases significantly ($\tau_D \geq 15$ ms). The photobleaching assumption is strongly supported by the fact that if the detection volume is moved a few microns in an immobilized insulin layer, the count rate shows an initial increase followed by a rapid decay.

Discussion of Adsorption Models

Several authors have studied surface adsorption of proteins using various methods, e.g., ellipisometry, reflectometry, Fourier transform infrared spectroscopy, pendant drop method, and total internal reflection fluorescence (36–38). A three-stage adsorption model has been suggested: (1) diffusion to the surface and conformational changes of the protein; (2) optimization of protein attachment by increasing interfacial contacts, resulting in a monolayer formation; (3) relaxation of the monolayer and buildup of a multilayer formation (36, 37). It is known that insulin forms condense films at the oil–water interface (6) at higher bulk concentration, and for some proteins (BSA and HSA) adsorption to the same interface was shown to involve structural rearrangement upon attachment (14). However, very little is known about the initial steps in the buildup of these protein films.

In this study the formation of a slow diffusion phase has, for the first time, been directly observed. A number of explanations for the abrupt phase change seen in Fig. 5 are discussed below.

Crowding has previously been observed by FCS to influence the diffusion constant significantly (10). In bulk 3D diffusion, the diffusion constant decreases at protein volume fractions of only a few percent. However, for higher bulk concentrations in our experiment ($C_{\text{bulk}} \geq 35$ nM), the surface concentration is virtually constant whereas formation of the slow phase occurs, and so it is not a result of an increased surface density alone.

Instead, formation of condensed, slow diffusion films at the oil–water interface must involve aggregation of some sort. Surfaces were previously shown to induce bulk fibrillation of insulin (12, 39) and it was suggested that misfolded monomers are formed at the surface and accordingly desorbed and polymerized to large fibril aggregates (12). If aggregation accounts for the decrease in self-diffusion constant, then the size of the diffusing species has to increase quite significantly. In this case, molecular brightness is expected to increase accordingly. Figure 7 shows brightness and diffusion time as a function of time. As shown, the molecular brightness remains constant during the transition into the slow phase regime.

The structure of the aggregates formed on different lipid substrates was examined by Sharp *et al.* (40). The structure found is a mixture of thin fractal branches and large round

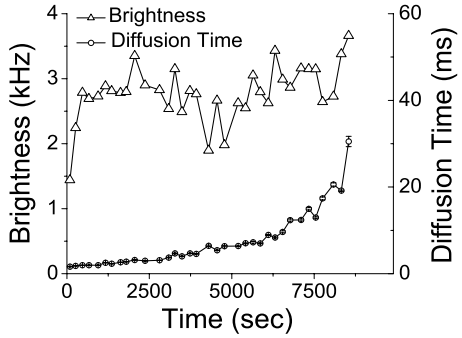

Fig. 7. The average brightness per molecule of the diffusing species is calculated using Eq. (8). During the measurement, brightness remains constant whereas diffusion time increases.

plaques. In a simulation study of 2D colloidal depletion, Cerda *et al.* (41) classified these two types of structures as fingerprints of diffusion limited aggregation (DLA) and reaction limited aggregation (RLA), respectively. In RLA, particles in close vicinity only aggregate with a certain probability that depends on the interaction potential, and the aggregates can relax to minimize the surface area. The clusters found are round and the dominant species is the monomer. In DLA, particles stick upon contact and form fractal networks where the monomer is no longer the dominant species. However, the morphology experimentally detected by Sharp *et al.* (40) suggests that aggregation does not occur as either the limiting cases of RLA or DLA. In our work the monomer is still the dominant species until the point where the phase shift occurs. The increase in diffusion time may be a result of a compartment formation by a fractal network formation.

CONCLUSIONS

We have demonstrated that FCS can give unique information about the dynamics of formation of protein layers at interfaces. A new phenomenon was observed: the molecules undergo an abrupt transition from a "fluid" surface into an almost immobile phase. We do not have a specific model to explain the transition.

In pharmaceutical formulation of proteins, the key goal is to maintain the protein in its active form. Aggregation is generally highly undesirable. It seems probable that the aggregation process leading to the formation of the rigid film at the interface involves changes to the protein that are difficult to reverse, such that the "liquid" form of the adsorbed layer is preferable. Our setup allows investigation of this process with some variations in excipients: buffer type, pH, salts, etc.

It is a considerable practical challenge in performing FCS experiments at liquid–liquid interfaces to establish a stable interface region within the working distance of a high numerical aperture objective, which is typically a few hundred microns. Of particular importance in the context of pharmaceutical formulation, planar oil–water interfaces are not stable in the presence of detergents. In our experiment, simple adsorption of minute oil drops to a cover slip was used, and we have so far not been able to use pharmaceutically relevant concentrations of surface-active substances. Investigations on the effect of detergents should use a different means of fixing the interface, such as the micropipette technique (6).

ACKNOWLEDGMENTS

Per Franklin Nielsen and Dorte Mørch Gundesen, Novo Nordisk A/S, are gratefully acknowledged for their assistance in the purification and analysis of FITC-labeled insulin. Jesper Donsmark was supported by a grant from the Danish Technical Research Council.

REFERENCES

1. W. Norde and J. Lyklema. Why proteins prefer interfaces? *J. Biomater. Sci., Polym. Ed.* **2**:183–202 (1991).
2. C. A. Haynes and W. Norde. Structures and stabilities of adsorbed proteins. *J. Colloid Interface Sci.* **169**:313–328 (1995).
3. C. O. Fagain. Understanding and increasing protein stability. *Biochim. Biophys. Acta* **1252**:1–14 (1995).
4. A. Kondo and T. Urabe. Relationships between molecular-states (conformation and orientation) and activities of alpha-amylase adsorbed on ultrafine silica particles. *Appl. Microbiol. Biotechnol.* **43**:801–807 (1995).
5. D. A. Parkins and U. T. Lashmar. The formulation of biopharmaceutical products. *Pharm. Sci. Technol. Today* **3**:129–137 (2000).
6. L. Jorgensen, D. H. Kim, C. Vermehren, S. Bjerregaard, and S. Froekjaer. Micropipette manipulation: a technique to evaluate the stability of water-in-oil emulsions containing proteins. *J. Pharm. Sci.* **93**:2994, 2004 (2004).
7. P. Schwille, J. Bieschke, and F. Oehlenschläger. Kinetic investigations by fluorescence correlation spectroscopy: the analytical and diagnostic potential of diffusion studies. *Biophys. Chem.* **66**:211–228 (1997).
8. R. Rigler, A. Pramanik, P. Jonasson, G. Kratz, O. T. Jansson, P. A. Nygren, S. Stahl, K. Ekberg, B. L. Johansson, S. Uhlen, M. Uhlen, H. Jornvall, and J. Wahren. Specific binding of proinsulin C-peptide to human cell membranes. *Proc. Natl. Acad. Sci.* **96**:13318–13323 (1999).
9. O. Hegener, L. Prenner, R. Runkel, S. L. Baader, J. Kappler, and H. Aberlein. Dynamics of beta$_2$-adrenergic receptor–ligand complexes on living cells. *Biochemistry* **43**:6190–6199 (2004).
10. R. Schmauder, T. Schmidt, J. P. Abrahams, and M. E. Kuil. Screening crystallisation conditions using fluorescence correlation spectroscopy. *Acta Crystallogr., D Biol. Crystallogr.* **58**:1536–1541 (2002).
11. H. Thurow and K. Geisen. Stabilisation of dissolved proteins against denaturation at hydrophobic interfaces. *Diabetologia* **27**:212–218 (1984).
12. V. Sluzky, J. A. Tamada, A. M. Klibanov, and R. Langer. Kinetics of insulin aggregation in aqueous solutions upon agitation in the presence of hydrophobic surfaces. *Proc. Natl. Acad. Sci. USA* **88**:9377–9381 (1991).
13. L. Jorgensen, C. Vermehren, S. Bjerregaard, and S. Froekjaer. Secondary structure alterations in insulin and growth hormone water-in-oil emulsions. *Int. J. Pharm.* **254**:7–10 (2003).
14. L. Jorgensen, M. van de Weert, S. Bjerregaard, C. Vermehren, and S. Frokjaer. Probing structural changes of proteins incorporated into water-in-oil emulsions. *J. Pharm. Sci.* **93**:1847–1859 (2004).
15. W. D. Lougheed, H. Woulfe-Flanagan, J. R. Clement, and A. M. Albisser. Insulin aggregation in artificial delivery systems. *Diabetologia* **19**:1–9 (1980).
16. J. Brange and L. Langkjaer. Insulin structure and stability. In Y. J. Wang and R. Pearlman Y. J. Wang R. Pearlman (eds.), *Stability and Characterisation of Protein and Peptide Drugs—-CaseHistories*, PlenumPress, NewYork, 1993, pp.315Y350.
17. J. Brange. *Stability of Insulin*, Kluwer Academic Publishers, Dordrecht, 1994.

18. T. Blundel, D. Dodson, D. Hodgkin, and D. Needham. Insulin: the structure in the crystal and its reflection in the chemistry and biology. *Adv. Protein Chem.* **26**:279–402 (1972).
19. J. Brange and A. Volund. *Adv. Drug Deliv. Rev.* **35**:307, 1999 (1999).
20. Y. Pocker and B. Biswas. Self-association of insulin and the role of hydrophobic bonding: a thermodynamic model of insulin dimerization. *Biochemistry* **20**:4354–4361 (1981).
21. N. G. Hentz, J. M. Richardson, J. R. Sportsman, and G. S. Sittampalam. Synthesis and characterization of insulin fluorescein derivatives for bioanalytical applications. *Anal. Chem.* **69**:4994–5000 (1997).
22. P. K. Smith, R. I. Krohn, G. T. Hermanson, A. K. Mallia, F. H. Gartner, M. D. Provenzano, E. K. Fujimoto, N. M. Goeke, B. J. Olson, and D. C. Klenk. Measurement of protein using bicinchoninic acid. *Anal. Biochem.* **150**:76–85 (1985).
23. K. Weisshart, V. Jungel, and J. R. Clement. The LSM 510 META–ConfoCor 2 system: an integrated imaging and spectroscopic platform for single-molecule detection. *Curr. Pharm. Biotechnol.* **5**:135–154 (2004).
24. K. Schätzel, M. Drewel, and S. Stimac. Photon correlation measurements at large lag times: improving statistical accuracy. *J. Mod. Opt.* **35**:711–718 (1988).
25. M. Eigen and R. Rigler. Sorting single molecules: application to diagnostics and evolutionary biotechnology. *Proc. Natl. Acad. Sci.* **1994**:5740, 1994 (1994).
26. R. Rigler, J. Widengren, and Ü Mets. Interactions and kinetics of single molecules as observed by fluorescence correlation spectroscopy. In O. Wolfbeis (ed.), *Fluorescence Spectroscopy*, Springer, Berlin, 1992, pp. 13–24.
27. J. Enderlein. Theoretical study of detection of a dipole emitter through an objective with high numerical aperture. *Opt. Lett.* **25**:634–636 (2000).
28. R. Rigler and J. Widengren. Ultrasensitive detection of single molecules as observed by fluorescence correlation spectroscopy. *BioScience* **3**:180–183 (1990).
29. P. Schwille. Fluorescence correlation spectroscopy and its potential for intracellular applications. *Cell Biochem. Biophys.* **40**:6036–6046 (2001).
30. J. Enderlein, I. Gregor, D. Patra, and J. Fitter. Art and artefacts of fluorescence correlation spectroscopy. *Curr. Pharm. Biotechnol.* **5**:155–161 (2004).
31. J. Widengren and R. Rigler. Mechanisms of photobleaching investigated by fluorescence correlation spectroscopy. *Bioimaging* **4**:149–157 (1996).
32. E. Kudryashova, A. Visser, and H. Jongh. Reversible self-association of ovalbumin at air–water interfaces and the consequences for the exerted surface pressure. *Protein Sci.* **14**:483–493 (2005).
33. K. Palo, U. Mets, S. Jager, P. Kask, and K. Gall. Fluorescence intensity multiple distributions analysis: concurrent determination of diffusion times and molecular brightness. *Biophys. J.* **79**:2858–2866 (2000).
34. J. Lagarias, J. Reeds, M. Wright, and P. Wright. Convergence properties of the Nelder–Mead simplex method in low dimensions. *SIAM J. Optim.* **9**(1):112–147 (1998).
35. T. Wohland, R. Rigler, and V. Vogel. The standard deviation in fluorescence correlation spectroscopy. *Biophys. J.* **80**:2987–2999 (2001).
36. M. Kleijn and W. Norde. The adsorption of proteins from aqueous solution on solid surfaces. *Heterog. Chem. Rev.* **2**:157–172 (2004).
37. C. J. Beverung, C. J. Radke, and H. W. Blanch. Protein adsorption at the oil/water interface: characterization of adsorption kinetics by dynamic interfacial tension measurements. *Biophys. Chem.* **81**:59–80 (1999).
38. S. H. Mollmann, J. T. Bukrinsky, S. Frokjaer, and U. Elofsson. Adsorption of human insulin and AspB28 insulin on a PTFE-like surface. *J. Colloid Interface Sci.* **286**:28–35 (2005).
39. L. Nielsen, R. Khurana, A. Coats, S. Frokjaer, J. Brange, S. Vyas, V. N. Uversky, and A. L. Fink. Effect of environmental factors on the kinetics of insulin fibril formation: elucidation of the molecular mechanism. *Biochemistry* **40**:6036–6046 (2001).
40. J. S. Sharp, J. A. Forrest, and R. A. Jones. Surface denaturation and amyloid fibril formation of insulin at model lipid–water interfaces. *Biochemistry* **41**:15810–15819 (2002).
41. J. C. Cerda, T. Sintes, C. M. Sorensen, and A. Chakrabati. Kinetics of phase transformations in depletion-driven colloids. *Phys. Rev., E* **70**:11405, 2004 (2004).